· Article · Advances in Polar Science
doi: 10.12429/j.advps.2024.0036 March 2025 Vol. 36 No. 1: 51-60

Conception and first results of the Russian National System of Background Permafrost Monitoring

Nikita E. DEMIDOV[1*], Oleg A. ANISIMOV[1,2], Mikhail A. ANISIMOV[1], Alexander L. BORISIK[1], Valerian E. GOLAVSKII[1], Maria A. GUSAKOVA[1], Alina V. GUZEVA[3], Alexander S. MAKAROV[1], Anton P. MOROZOV[1], Irina Yu. SOLOVYANOVA[1], Alexander A. STEPANETS[1], Yuriy V. UGRUMOV[1] & Daria K. ZAITSEVA[1]

[1] Arctic and Antarctic Research Institute, St. Petersburg 199397, Russia;
[2] State Hydrological Institute of Roshydromet, St. Petersburg 199053, Russia;
[3] St. Petersburg Federal Research Center of RAS—Institute of Limnology RAS, St. Petersburg 196105, Russia

Received 11 October 2024; accepted 22 January 2025; published online 30 March 2025

Abstract In 2022, the Russian Federation commenced development of a national system for permafrost monitoring. The conceptual design of this system reflects three objectives: (1) to collect data on the impact of climate change on permafrost, (2) to provide data for evaluation of climate–permafrost feedback, and (3) to provide input to a model-based permafrost data assimilation system. It is intended that the system will eventually consist of 30 active layer monitoring sites and 140 boreholes situated near existing weather stations. As of October 2024, the network comprised 38 sites spanning from the High Arctic islands to the Altai Mountains and across western and eastern Siberia. Among these sites, the lowest recorded temperature at the depth of zero annual amplitude is −11.3℃ and the minimum active layer thickness is 0.3 m, as observed on the New Siberian Archipelago. In most boreholes, a positive vertical temperature gradient exists below the depth of zero annual amplitude, indicative of ongoing warming of the upper permafrost layer attributable to climate change. The annual maximum active layer thickness is observed in September with only two exceptions: at the High Arctic sites on Franz Josef Land and Wiese Island and in the low-latitude Sayan Mountain region, where maximum thawing is observed at the end of August. Talik was found in boreholes in Salekhard and Altai where the upper boundary of the permafrost is located at depth of 6–10 m.

Keywords **monitoring**, **climate change**, **weather station**, **permafrost**, **active layer**

Citation: Demidov N E, Anisimov O A, Anisimov M A, et al. Conception and first results of the Russian National System of Background Permafrost Monitoring. Adv Polar Sci, 2025, 36(1): 51-60, doi: 10.12429/j.advps.2024.0036

1 Introduction

Permafrost is a distinct feature of high-latitude and high-elevation environments. According to Gruber (2012), it occupies approximately 25% of the land area in the Northern Hemisphere and more than 60% of the Russian territory. The state of permafrost is best characterized by the ground temperature at the depth of zero annual amplitude and by the thickness of the upper-most layer of seasonal thawing, called the active layer thickness (ALT).

In Russia, data on permafrost temperature and ALT were historically available from four different sources (Anisimov and Zimov, 2021). The longest data records come

* Corresponding author. ORCID: 0000-0002-3462-7747. E-mail: nikdemidov@mail.ru

from a subset of 146 Russian weather stations located in permafrost regions. Daily ground temperature measurements are taken at 12 standardized levels down to the depth of 3.2 m below the surface. Most of these data are available on the data portal (https://www.meteo.ru), and they represent the only continuous and long-term permafrost observations conducted routinely by the Federal Service for Hydrometeorology and Environmental Monitoring of the Russian Federation (Roshydromet). Importantly, these permafrost data are complemented by a full set of atmospheric meteorological parameters measured at corresponding weather stations.

In the 1990s, the academic permafrost community launched the Circumpolar Active Layer Monitoring (CALM) program, whereby end-of-season thaw depth is measured once annually by mechanical probing at nodes in a regular grid (usually, 121 probes per site). Currently, the CALM program includes more than 230 sites, many of which are operated on a volunteer basis. Data are freely available at the portal (https://www2.gwu.edu/~calm/). Of the 68 CALM sites that have been operating in Russia in various years, only approximately 20 sites have long-term records dating back to the 1990s.

In parallel to the CALM program, the international Thermal State of Permafrost (TSP) project was launched to conduct ground temperature observations in boreholes. More than 1360 TSP boreholes have been instrumented, including 384 in Russia. Data recorded at many TSP sites are available via the internet (https://gtnp.arcticportal.org). The depth of the TSP boreholes varies from <10 m to >100 m. Taken together, the TSP and CALM observations comprise the Global Terrestrial Network for Permafrost (GTN-P). In Russia, permafrost observations have also been conducted in association with research projects at 35 plots in Northern Europe and Siberia; however, these data are not in the public domain.

Increasing evidence based on GTN-P data shows that warming and thawing of permafrost have accelerated in past decades (Biskaborn et al., 2019), raising public concerns regarding the infrastructure built upon frozen ground and the potential impact on the global climate through enhanced emission of greenhouse gases. The total value of the infrastructure at risk in Russian permafrost regions is much higher than that elsewhere in the Arctic (Badina and Pankratov, 2021; Porfiriev et al., 2021). Potential economic and ecological damage calls for the development of a nationwide monitoring network that can provide robust data on permafrost changes under various geological, bio-physiographic, and climatic conditions. For several reasons, existing GTN-P observations do not serve this goal effectively.

First, GTN-P observations are strongly project-driven. Consequently, measurements are often made over short temporal intervals and at locations that might not be representative of environmental conditions, but rather reflect historical or logistical constraints. The representativeness of measurements with respect to topographical, geological, and bioclimatic conditions is commonly not evaluated. Thus, existing observations do not support comprehensive evaluation of the full spatiotemporal pattern of the permafrost state, particularly in the southernmost sporadic permafrost zone, where permafrost has already thawed at many locations due to climate change (Biskaborn et al., 2019; Romanovsky et al., 2010).

Another constraint is that GTN-P observations do not include auxiliary meteorological data, complicating the attribution of observed permafrost variations and long-term changes to specific factors, e.g., climate change or variations in precipitation regime. While public perception most commonly associates permafrost warming and thawing with rise in air temperature, a case study at Chersky in the Kolyma Lowland demonstrated that the increase in snow depth might play a more important role (Anisimov and Zimov, 2021). Thicker snow pack increases the difference between the air temperature and the annual ground temperature by 3–5℃, leading to abrupt increase in ALT and even to permafrost thawing at selected locations.

There are also notable ‘blank spots’ where permafrost monitoring has yet to be undertaken, and where the general geocryological conditions have not been investigated. One of these blank spots is the Arctic archipelagos along the Northern Sea Route. Different approaches and different measuring equipment are used at existing sites, meaning that it is extremely difficult to combine the obtained data into a single database and to apply uniform processing and analysis algorithms.

In 2022, the Russian government decided to develop the Russian National System for Background Permafrost Monitoring (RNS BPM). The system will be organized and operated by the Arctic and Antarctic Research Institute of Roshydromet. The construction of this network is expected to be completed by 2025. In this paper, we present the conceptual design of the monitoring system and provide the first results based on data obtained from 38 boreholes.

2 Methods

The conceptual design of the RNS BPM reflects three objectives: (1) to collect data on the impact of climate change on permafrost with particular focus on identifying the tipping points of permafrost thawing, (2) to provide data for evaluation of climate–permafrost feedback through the emission of greenhouse gases from thawing permafrost, and (3) to provide input to a model-based permafrost data assimilation system and thus harmonize permafrost research methodologies based on analysis of observations and mathematical modeling.

Ultimately, the monitoring network is intended to consist of 140 boreholes, most of which will be drilled and instrumented in close proximity to existing weather stations at locations representing a wide range of permafrost, geological, bio-climatic, and topographic conditions. Thus,

temperature observations from the boreholes will be supplemented by a full set of standard meteorological data from the weather stations and metadata characterizing local conditions, including soil type and properties.

Similar to weather stations, RNS BPM monitoring sites are located in undisturbed environments at a sufficient distance from engineering structures that could distort the natural temperature field of the soil. This is the fundamental difference between background monitoring by geotechnical monitoring systems, which are aimed at studying the temperature field in the zone of interaction between infrastructures and frozen soils. The location of monitoring sites must also represent the most common permafrost conditions within the area (e.g., avoiding installation in local taliks and pingos).

The main parameters measured at RNS BPM sites are permafrost temperature and ALT. These parameters are consistent with the recommendations of the World Meteorological Organization (WMO) in the field of permafrost monitoring (Burgess et al., 2000). Conceptually, the RNS BPM is intended to comprise 140 permafrost temperature monitoring sites and 30 ALT sites. The RNS BPM is based on the principle that all temperature monitoring boreholes have common depth and equipment. Moreover, the ALT sites are also unified. The depth of the thermometric boreholes is 25 m. This depth makes it possible to cover the heat turnover layer in which annual temperature fluctuations occur, and to measure the temperature at the depth of zero annual amplitude. The standard 25-m depth of the boreholes allows measurement of the temperature gradient below the annual heat cycle layer, thereby helping to elucidate whether the upper part of the permafrost is in a warming cycle. When choosing the placement of thermistors on the string, the standards of Roshydromet (down to the depth of 3.2 m) and the standards for temperature measurements in boreholes during engineering–geocryological research in Russia were considered. The thermistor string contains 32 sensors for measuring temperatures at the following depths: 0, 0.2, 0.4, 0.5, 0.6, 0.8, 1.0, 1.2, 1.5, 1.6, 2.0, 2.4, 2.5, 3.0, 3.2, 3.5, 4.0, 4.5, 5.0, 6.0, 7.0, 8.0, 9.0, 10.0, 12.0, 14.0, 16.0, 18.0, 20.0, 22.0, 24.0, and 25.0 m. Existing boreholes are instrumented using thermistor strings from MSU-Geophysics LLC (Russia) and Marlin-Yug LLC (Russia), which are capable of measuring temperature with a resolution of 0.01℃ and accuracy of ±0.1℃. For the first time in the national practice of permafrost research, the system works in near-real time. Observational data are transferred automatically (at 6-h intervals) using a satellite-based data transmission system. This makes it possible to quickly display data from all permafrost monitoring sites using the information system of the RNS BPM. It is intended that the information system will be publicly accessible after the creation of all 140 monitoring sites.

To preserve the undisturbed state of the soil when organizing monitoring sites, drilling is performed using portable small-sized rigs (or heavy-duty rigs in winter) or from special flooring. Thermometric equipment is lowered into a narrow plastic tube and the annular space is filled with local soil. This is performed to minimize the influence of convective heat exchange due to air movement. The steel conductor pipe contains the logger and the satellite transmitter. Above the surface, the steel pipe is insulated by an external plastic pipe, which contains a heat insulator to prevent the influence of air temperature on the near-surface thermistors (Figure 1).

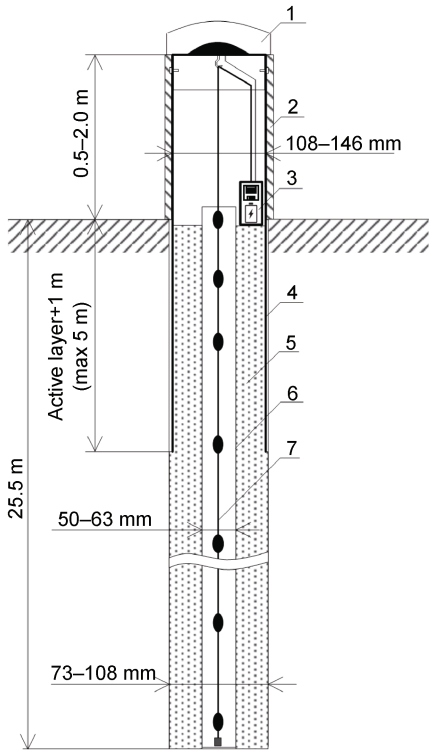

Figure 1 Construction of a permafrost temperature monitoring borehole: 1, downlink transmitter; 2, heat insulator in external plastic pipe; 3, logger and battery; 4, steel pipe; 5, local soil; 6, plastic tube; 7, thermistor string.

The thickness of the seasonally thawed layer at ALT sites is determined using the method applied in the CALM program (Brown et al., 2000). In recognition of the large areas of mountainous regions in the country, which can make it difficult to find suitable sites, ALT sites (50 × 50 m) are smaller than CALM sites (100 × 100 m). During the period of maximum thawing, the thickness of the seasonally thawed layer is measured at 121 points with a step of 5 m.

The concept of the RNS BPM also involves the creation of predictive assessments of the dynamics of permafrost conditions based on numerical modeling. For this purpose, during the organization of monitoring sites, core samples are taken for subsequent laboratory analysis of soil moisture in terms of water or ice content, thermal conductivity, heat capacity, and freezing point. Frozen samples are stored in the core storage at the Arctic and Antarctic Research Institute at sub-zero temperatures to allow for additional analysis in the future.

3 Results

At the time of writing, 38 boreholes have been drilled and instrumented close to operating weather stations. Geographically, they span the region 49.7°N–80.6°N, 14.2°E–178.6°W (Figure 2). The borehole on Svalbard Archipelago is located near the Barentsburg weather station (WMO index no.: 20107) in West Spitsbergen. Of the 38 boreholes currently established, 14 have produced year-long data records beginning in autumn 2023. For these boreholes, the depth of zero annual amplitude (H_0) has been calculated (Table 1), together with the temperature at this depth (T_0), the mean annual ground surface temperature (T_{MGS}), and the linear temperature gradient ($GRADT_{BTO}$) at depth intervals from T_0 to 25 m. For all boreholes listed in Table 1, the ground temperature (T_{25}) at 25 m is presented, together with the ALT, estimated by interpolating the depth of the 0℃ isotherm. The corresponding date of maximum ALT is also presented. For three boreholes with a deepened upper boundary of permafrost, the thickness of talik above the permafrost is presented instead of the ALT.

Climatic characteristics calculated from observational data recorded at each corresponding weather station are also presented in Table 1. They include the mean annual air temperature (T_{MA}) for the period 2019–2023, the mean annual air temperature trend ($GRADT_{MA}$) for period 1994–2023, the annual precipitation trend ($GRADP_{MA}$) for the same period, and the mean annual air temperature (T_Y) for the period from 31 August 2023 to 1 September 2024.

Figure 3 illustrates the lithology and ground thermal characteristics (annual minimum, mean, and maximum temperatures) at eight boreholes from autumn 2023 to autumn 2024, representing an annual measurement cycle. Dots above the plots indicate annual minimum, mean, and maximum air temperatures measured at adjacent weather stations during the corresponding year-long period.

4 Discussion

4.1 Monitoring approach

The first annual cycle of measurements demonstrated the efficiency of the equipment used at RNS BPM sites. The absence of failure in the operation of data loggers and the satellite-based data transmission system enabled the calculation of mean annual parameters for the permafrost thermal state. It must be noted that borehole locations represent a broad range of climatic conditions, including the extremely cold winter environment of Oymyakon (−58℃ on 5 December 2023). At all 14 boreholes with an annual cycle

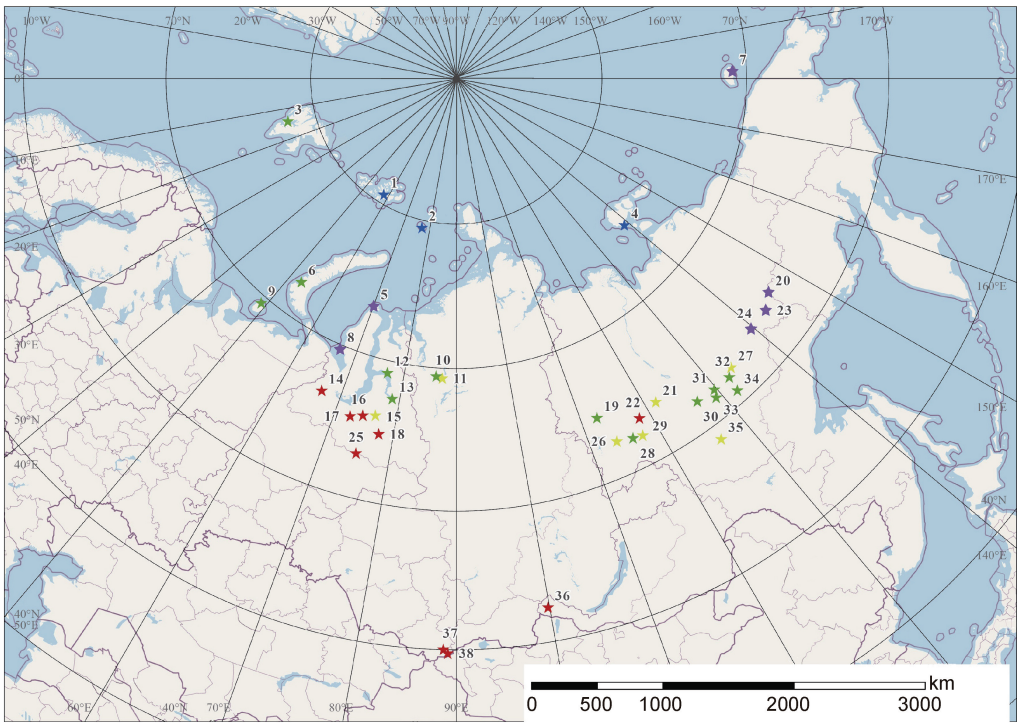

1 im E.T. Krenkelya (o. Hejsa) (20046)
2 Ostrov Vize (20069)
3 Barentsburg (20107)
4 Proliv Sannikova (21535)
5 im. M.V. Popova (o. Belyj) (20667)
6 Malye Karmakuly (20744)
7 Ostrov Vrangelya (21982)
8 Marresalya (23032)
9 Kolguev Severnyj (22095)
10 Dudinka (23074)
11 Noril'sk (23078)
12 Antipayuta (23058)
13 Tazovskij (23256)
14 Salekhard (23330)
15 Novyj Urengoj (airport) (23358)
16 Pangody (23443)
17 Nadym (23445)
18 Tarko-Sale (23552)
19 Habardino (24525)
20 Delyankir (24691)
21 Vilyujsk (24641)
22 Nyurba (24639)
23 Ojmyakon (24688)
24 Vostochnaya (24679)
25 Noyabr'sk (23657)
26 Mirnyj (24726)
27 Ytyk-Kyuyol' (24766)
28 Krestyah (24737)
29 Suntar (24738)
30 Berdigestyah (24758)
31 Churapcha (24768)
32 Yakutsk (24959)
33 Pokrovsk (24856)
34 Amga (24962)
35 Tommot (31005)
36 Orlik (29998)
37 Kosh-Agach (36259)
38 Tashanta (36458)

Figure 2 Map of the 38 weather stations equipped with temperature monitoring boreholes. The legend presents the name and WMO index number of each weather station.

Table 1 Climatic and ground thermal characteristics for RNS BPM stations

Station, WMO index	Lat., long., elevation	T_0/℃, T_{25}/℃	ALT/m, Date [DD-MM-YYYY]	H_0/m	GRADT$_{BTO}$, /(℃·m^{-1})	T_{MGS}/℃	T_{MA}/℃, T_Y/℃	GRADT$_{MA}$/(℃·a^{-1})	GRADP$_{MA}$/(mm·a^{-1})
im E.T. Krenkelya (o. Hejsa), 20046	80.6°N, 58.0°E, 21 m	−9.1, −9.3	0.80, 23-08-2024	15.3	−0.027	−7.8	−9.5, −9.2	0.15	1.4
Ostrov Vize, 20069	79.4°N, 76.9°E, 10 m	−10.4, −10.9	0.61, 20-08-2024	19.3	−0.071	−8.8	−10.0, −9.4	0.20	1.4
Barentsburg, 20107	78.0°N, 14.2°E, 75 m	−3.2, −3.3	1.45, 06-09-2024	5.8	−0.000	−3.0	−2.9, −2.8	0.12	2.9
Proliv Sannikova, 21535	74.6°N, 138.9°E, 15 m	−11.3, −11.2	0.31, 02-09-2024	22.0	−0.011	−12.1	−12.3, −12.3	0.10	−6.2
im. M.V. Popova (o. Belyj), 20667	73.3°N, 70.0°E, 4 m	−5.2, −6.8	0.97, 06-09-2024	9.7	−0.100	−3.9	−7.3, −7.2	0.17	2.3
Malye Karmakuly, 20744	72.4°N, 52.7°E, 18 m	-, −2.4	5.77, 20-09-2024	-	-	-	−2.2, −2.6	0.14	0.3
Ostrov Vrangelya, 21982	70.9°N, 178.6°W, 18 m	-, −7.3	0.77, 02-09-2024	-	-	-	−8.2, −9.5	0.11	0.6
Marresalya, 23032	69.7°N, 66.8°E, 24 m	−4.4, −5.4	1.31, 22-09-2024	9.3	−0.065	−3.5	−5.1, −5.7	0.12	3.9
Kolguev Severnyj, 22095	69.5°N, 49.0°E, 24 m	-, −2.2	2.30, 30-09-2024	-	-	-	−0.4, −1.7	0.12	−3.0
Dudinka, 23074	69.4°N, 86.1°E, 90 m	-, −2.0	2.37, 10-09-2024	-	-	-	-	0.12	-
Noril'sk, 23078	69.3°N, 88.2°E, 65 m	−1.6, −0.5	1.21, 01-09-2024	12.8	0.092	−5.1	−6.5, −6.9	0.10	3.0
Antipayuta, 23058	69.1°N, 76.8°E, 2 m	-, −4.5	0.92, 12-09-2024	-	-	-	−6.7, −7.1	0.15	5.5
Tazovskij, 23256	67.4°N, 78.7°E, 26 m	−2.8, −3.0	1.45, 27-09-2024	16.7	−0.029	−1.2	−5.4, −6.3	0.12	−4.9
Salekhard, 23330	66.5°N, 66.6°E, 50 m	0.0, 0.0	9.80*	9.8	−0.003	2.5	−3.4, −4.5	0.09	0.5
Novyj Urengoj (airport), 23358	66.0°N, 76.5°E, 58 m	−0.6, −1.3	0.77, 19-09-2024	7.4	−0.039	−2.0	−4.5, −5.4	0.13	4.5
Pangody, 23443	65.8°N, 74.5°E, 50 m	-, −0.1	1.24, 19-09-2024	-	-	-	−3.9, −4.9	0.10	9.1
Nadym, 23445	65.4°N, 72.6°E, 14 m	−0.5, −0.3	1.06, 21-09-2024	11.0	0.012	−0.3	−2.9, −4.0	0.10	1.3
Tarko-Sale, 23552	64.9°N, 77.8°E, 27 m	-, −0.2	1.25, 26-09-2024	-	-	-	−3.0, −3.7	0.10	3.3
Habardino, 24525	64.6°N, 112.5°E, 251 m	-, −2.8	2.27, 22-09-2024	-	-	-	−9.3, −9.6	0.05	-
Delyankir, 24691	63.8°N, 145.6°E, 800 m	-, −7.4	0.79, 10-09-2024	-	-	-	−14.6, −14.4	0.02	-
Vilyujsk, 24641	63.7°N, 121.6°E, 111 m	-, −0.6	3.09, 03-09-2024	-	-	-	−6.3, −6.7	0.08	0.3
Nyurba, 24639	63.2°N, 118.3°E, 119 m	-, −0.2	1.97, 11-09-2024	-	-	-	−6.4, −6.7	0.07	−6.9
Ojmyakon, 24688	63.2°N, 143.1°E, 740 m	−5.6, −5.8	1.45, 17-09-2024	20.4	−0.031	−7.2	−14.1, −12.2	0.06	1.0
Vostochnaya, 24679	63.2°N, 139.6°E, 1286 m	−6.2, −6.4	2.15, 14-09-2024	22.5	−0.077	−9.8	−12.2, −14.1	0.05	1.6
Noyabr'sk, 23657	63.1°N, 75.2°E, 131 m	-, 0.4	1.26, 14-09-2024	-	-	-	−2.2, −3.0	0.10	4.0
Mirnyj, 24726	62.5°N, 114.0°E, 352 m	-, −1.5	2.98, 17-09-2024	-	-	-	−5.1, -	0.08	−0.8
Ytyk-Kyuyol', 24766	62.3°N, 133.5°E, 152 m	-, −1.8	3.03, 30-09-2024	-	-	-	−9.6, −9.7	0.05	-
Krestyah, 24737	62.2°N, 116.1°E, 140 m	-, −2.0,	2.64, 16-09-2024	-	-	-	−5.7, −5.8	0.06	-
Suntar, 24738	62.1°N, 117.6°E, 138 m	-, −1.0	2.91, 29-09-2024	-	-	-	−4.7, −5.0	0.08	0.3
Berdigestyah, 24758	62.0°N, 126.7°E, 231 m	-, −2.4	1.42, 14-09-2024	-	-	-	−7.8, −8.3	0.06	-
Churapcha, 24768	62.0°N, 132.6°E, 186 m	-, −2.2	1.94, 15-09-2024	-	-	-	−8.5, −8.8	0.08	1.4
Yakutsk, 24959	62.0°N, 129.6°E, 101 m	-, −2.5	1.72, 15-09-2024	-	-	-	−6.9, −7.2	0.07	0.3
Pokrovsk, 24856	61.4°N, 129.1°E, 115 m	-, −2.2	2.74, 25-09-2024	-	-	-	−7.7, −7.8	0.06	0.2
Amga, 24962	60.9°N, 131.9°E, 146 m	−2.3, −2.4	1.75, 15-09-2024	16.0	−0.018	−2.9	−8.4, −8.6	0.06	−0.3
Tommot, 31005	58.9°N, 126.2°E, 284 m	-, −0.9	1.32, 02-09-2024	-	-	-	−5.8, −6.2	0.01	-
Orlik, 29998	52.5°N, 99.8°E, 1376 m	-, −0.3	2.37, 26-08-2024	-	-	-	−3.3, −2.9	0.02	−0.1
Kosh-Agach, 36259	50.0°N, 88.6°E, 1759 m	-, −0.2	8.93*	-	-	-	−3.4, -	−0.01	1.6
Tashanta, 36458	49.7°N, 89.1°E, 2107 m	-, 0.5	5.90*	-	-	-	−2.6, −0.5	-	-

Notes: "*" indicating the thickness of talik above permafrost; "-" indicating no data.

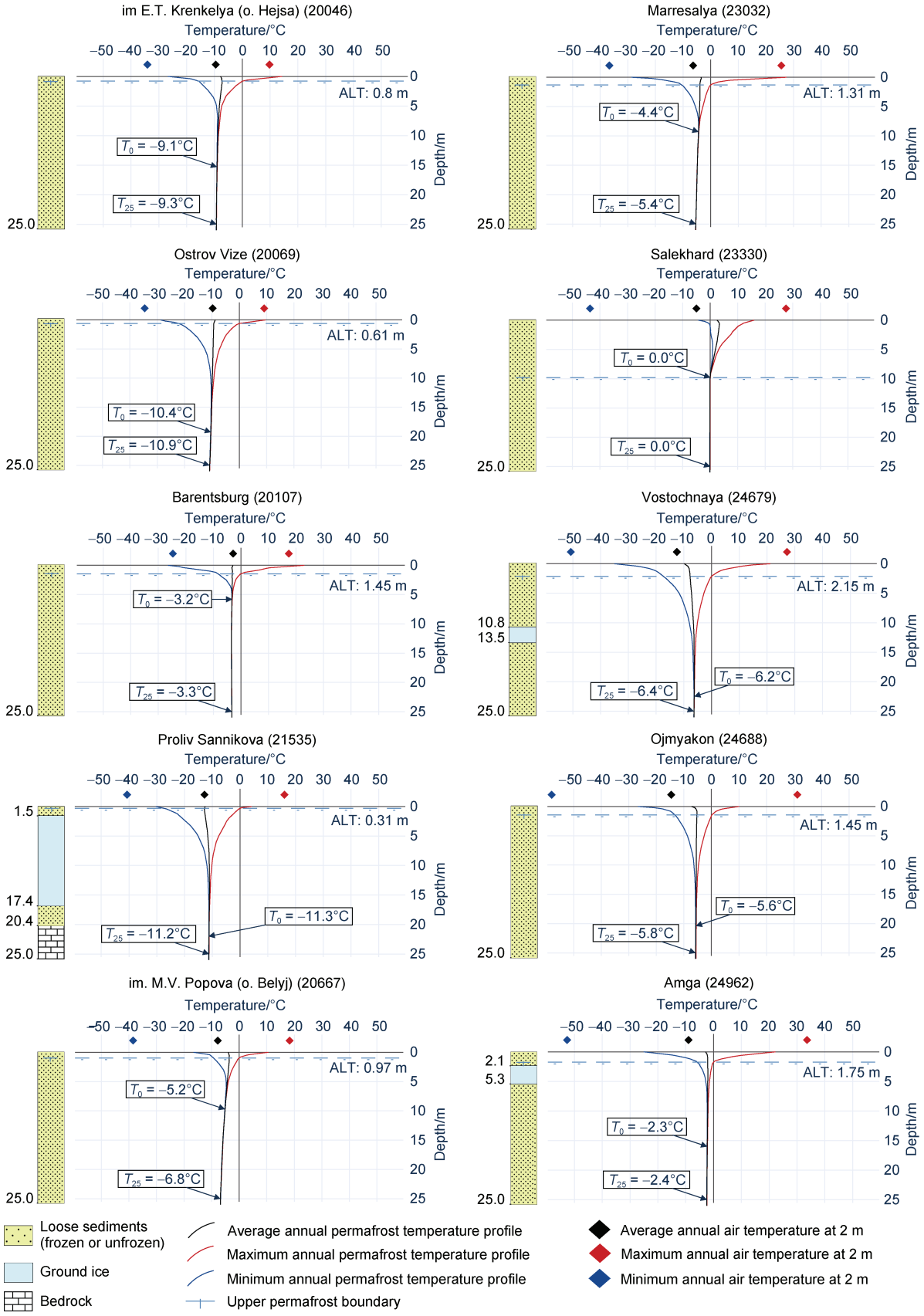

Figure 3 Lithology and ground thermal characteristics of eight boreholes with an annual cycle of measurements from autumn 2023 to autumn 2024. The name and WMO index number of the weather stations are presented above the plots.

of measurements, the depth of zero annual amplitude is situated above the 25-m level (Table 1). This finding indicates that for most of the 140 planned RNS BPM boreholes, the depth of zero annual amplitude is likely to remain within the 25-m depth of the borehole. The linear temperature gradient at depth intervals from zero annual amplitude to 25 m was also calculated for all 14 boreholes (Table 1). Thus, on the basis of analysis of the yearly measurements, we propose that a borehole with depth of 25 m is the optimal solution for the RNS BPM. The satellite-based data transmission system supports provision of near-real time data on ALT dynamics through interpolation of the depth of the 0 ℃ isotherm. This will help in selecting the day most appropriate for obtaining measurements of the maximum ALT using a graduated metal rod at RNS BPM monitoring sites. In three boreholes, a deepened upper boundary of permafrost was observed. Thus, the 25-m-deep boreholes enable observation of any change in permafrost boundary depth, together with determination of potential transition from seasonal thawing to talik formation in other boreholes with high-temperature permafrost.

4.2 Regional specifics of the permafrost thermal state

The data already obtained contribute to updating the regional data compilation of permafrost thermal state data in Russia, which is still represented primarily by the geocryological map of the USSR (Yershov, 1996) and associated scientific publications (Romanovsky et al., 2010). Seven of the boreholes provide data characterizing the thermal state of permafrost on the High Arctic archipelagos and islands along the Northern Sea Route (Figure 2). Because not all boreholes have been in operation long enough to provide an annual measurement cycle, for comparison, we use values of T_0 and T_{25}, which are closely aligned (Table 1) and approximate ground temperature at the base of the seasonal temperature fluctuation layer. In the western Eurasian High Arctic, the influence of Atlantic heat flux results in relatively warm permafrost: T_0 on the Spitsbergen Archipelago is −3.2 ℃, T_{25} on Novaya Zemlya is −2.4 ℃, and T_{25} on Kolguev Island is −2.2 ℃. The influence of the Atlantic on permafrost temperature extends even as far as Franz Josef Land. The annual cycle of measurements at the borehole on Hejsa Island (80.6°N), the northernmost temperature monitoring borehole in Eurasia, revealed a T_0 value of −9.1 ℃. On Wiese Island (east of Franz Josef Land) and the New Siberian Islands, the latitude is lower but T_0 is −10.4 and −11.3 ℃, respectively. Influence from the Pacific heat flux results in higher ground temperatures on Wrangel Island (T_{25} = −7.3 ℃).

Twelve boreholes of the RNS BPM were drilled in northern Western Siberia. They show how the thermal state of permafrost changes with distance from Belyj Island in the north of the Yamal Peninsula, with T_0 increasing from −5.7 ℃ to between −0.6 and 0 ℃ in the region of the cities of Salekhard, Nadym, and Novy Urengoy (Yamal–Nenets Autonomous Area). In Salekhard the RNS BPM borehole revealed a deepened upper boundary of permafrost at the depth of 9.8 m. The southernmost borehole for monitoring temperature in Western Siberia was drilled at 63.1°N near Noyabrsk city, where the permafrost base was found at the depth of 21.9 m. Temperatures in the Norilsk industrial region are lower than background temperatures near the above-mentioned cities in the Yamal–Nenets Autonomous Area: T_0 = −1.6 ℃ in Norilsk and T_{25} = −2.0 ℃ in Dudinka.

The region of the Republic of Yakutia that lies south of the Arctic Circle is also already covered by a network of 16 RNS BPM boreholes. The lowest permafrost temperatures are found in the east of Yakutia at the Delyankir (T_{25} = −7.4 ℃), Vostochnaya (T_0 = −6.2 ℃), and Ojmyakon (T_0 = −5.6 ℃) weather stations. In the remaining areas of the territory, permafrost temperatures are relatively high with T_{25} ranging from −3.8 to −0.2 ℃. In Yakutsk, the city with the largest population among those cities within the permafrost zone, T_{25} is −2.5 ℃.

The three boreholes drilled in the Altai–Sayan are representative of mountain permafrost with temperatures near to 0 ℃. Our data show that permafrost is degrading in the Chuya Lowland, where boreholes at 1759 m a.s.l. in Kosh–Agach and at 2109 m a.s.l. in Tashanta revealed a deepened upper boundary of permafrost at depth of 8.93 and 5.9 m, respectively, below the depth of seasonal freezing/thawing. In Tashanta, the permafrost base was also detected at the depth of 22.1 m. By contrast, data from the borehole at the Orlik weather station, which is 1376 m a.s.l., indicated that there is no talik and that the permafrost is characterized by a T_{25} value of −0.3 ℃.

The lowest mean annual temperature of permafrost was measured in the High Arctic: T_0 = −11.3 ℃ on the islands of the New Siberian Archipelago and T_0 = −10.4 ℃ on Wiese Island. In the High Arctic, the difference between the mean annual air temperature, T_{MGS}, and mean temperature at depth of zero annual amplitude is negligible (Figure 3). Mean annual air temperature in both Delyankir and Oymyakon in continental Yakutia is lower than that in the High Arctic (Table 1). In Delyankir and Oymyakon, T_{MGS} is markedly higher than the mean annual air temperature. Mean annual temperature at the permafrost surface is also higher than T_{MGS} in this part of Yakutia. One of the main (but not the only) factors, leading to this difference between the High Arctic and continental regions, is snow. Owing to persistent strong winds in the Arctic, snow is denser, has higher thermal conductivity, and less effectively insulates the surface from the cold air. By contrast, in the anomalously cold regions of continental Yakutia, winter weather is controlled by the Siberian anticyclone. Strong winds are rare, which is why snow pack has low density and low thermal conductivity, preventing the underlying surface from cooling. As illustrated in Figure 3, the absolute minimum air temperature

at the Oymyakon weather station is lower than that at the Proliv Sannikova weather station (New Siberian Archipelago). However, the absolute minimum ground surface temperature at Proliv Sannikova is lower than that at Oymyakon. This effect is explained by the ability of the snow cover in Oymyakon to effectively insulate the ground surface against cooling.

The maximum ALT estimated by interpolating the depth of the 0 ℃ isotherm in 2024 was found on Novaya Zemlya, where it reached 5.8 m (maximum thaw on 20 September 2024). The ALT exceeds 2 m on Kolguev Island in the Barents Sea (2.3 m on 30 September 2024), in the region of the mouth of the Yenisei River where the city of Dudinka is located (2.37 m on 10 September 2024), in Orlik in the Sayan Mountain region (2.37 m on 26 August 2024), and at several stations in Yakutia: Habardino (2.27 m on 22 September 2024), Vilyujsk (3.09 m on 3 September 2024), Vostochnaya (2.15 m on 14 September 2024), Mirnyj (2.98 m on 17 September 2024), Ytyk–Kyuyol′ (3.03 m on 30 September 2024), Krestyah (2.64 m on 16 September 2024), and Suntar (2.91 m on 29 September 2024). The minimum ALT value in 2024 was found on the New Siberian Archipelago, where it reached 31 cm on 2 September 2024. On other islands of the High Arctic, except Spitsbergen, the ALT values were also among the smallest.

4.3 Dependence between climate and permafrost thermal parameters

Figure 4 illustrates that the trend of mean annual air temperature for the period 1994–2023 at 37 weather stations was positive. The only exception is Kosh-Agach in the Altai region, where the trend of air temperature over the same period was negative. Statistically significant dependence was found between the trend of air temperature and the latitude of the monitoring area (correlation coefficient r = 0.84), whereas the trend of mean annual precipitation does not depend on latitude (r = 0.03) (Figure 5).

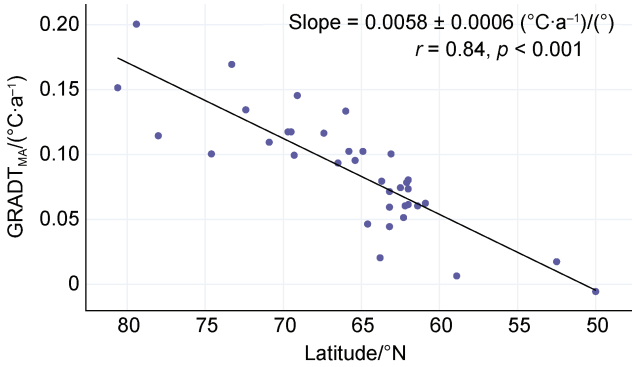

Figure 4 Scatter plot of latitude–mean annual air temperature ($GRADT_{MA}$) for the period 1994–2023 for 38 RNS BPM weather stations. Legend presents values of the slope coefficient, correlation coefficient (r), and significance level (p-value).

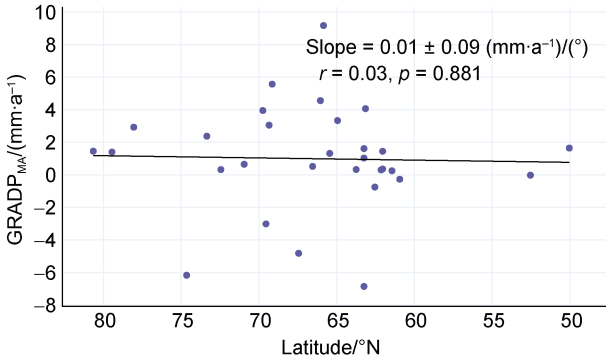

Figure 5 Scatter plot of latitude–mean annual precipitation ($GRADP_{MA}$) for the period 1994–2023 for 38 RNS BPM weather stations. Legend presents values of the slope coefficient, correlation coefficient (r), and significance level (p-value).

The dependence between ALT and T_{25} (this temperature characteristic was taken because data already exist for 38 boreholes, while T_0 has been calculated for only 14 boreholes) demonstrates the obvious effect of ALT thinning in areas with low permafrost temperature (Figure 6). The correlation coefficient is 0.53 when considering all boreholes except the Novaya Zemlya borehole, where the active layer has anomalous thickness (5.8 m) that can be explained by the presence of bedrock with high thermal conductivity and low ice content close to the surface. Figure 6 shows that the deviation of the points from the linear regression line increases with rising ground temperature. This increase might be attributable to the increasing effect of local environmental factors, particularly vegetation and soil hydrology, on ALT in high-temperature permafrost regions. For example, the presence of peat cover can substantially reduce ALT, even in high-temperature permafrost.

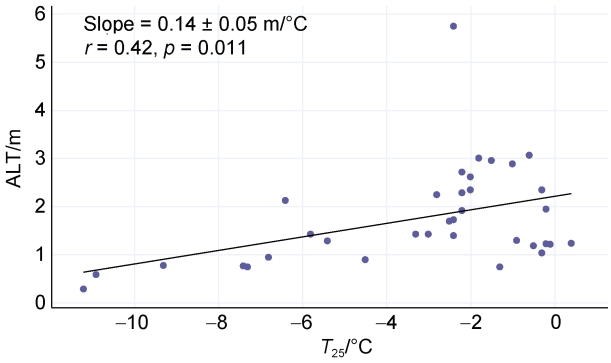

Figure 6 Scatter plot of ground temperature (T_{25}) at depth of 25 m–ALT for 38 RNS BPM weather stations. Legend presents values of the slope coefficient, correlation coefficient (r), and significance level (p-value).

Figure 7 illustrates the dependence between ALT and T_Y. It is evident that most of the blue dots lie below the regression line. This effect of decrease in ALT compared with the prediction of the regression line might be explained

by the specific climate on Arctic islands, the main features of which are cold, cloudy, and short summers. The only dot situated above the regression line corresponds to the Novaya Zemlya borehole, where ALT is abnormally thick owing to proximity to the surface bedrock.

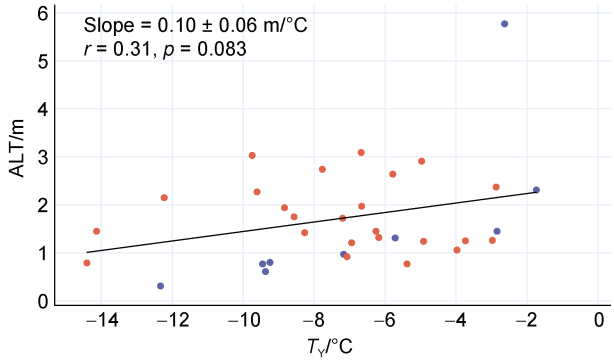

Figure 7 Scatter plot of mean annual air temperature (T_Y) for the period 31 August 2023 to 1 September 2024 –ALT for 38 RNS BPM weather stations. Blue dots correspond to weather stations on Arctic islands. Legend presents values of the slope coefficient, correlation coefficient (r), and significance level (p-value).

Figure 8 illustrates the dependence between T_{25} and mean annual air temperature (T_{MA}) for the period 2019–2023. The correlation coefficient between these two parameters is r = 0.69. This plot demonstrates that local factors might cause notable variation in the ground temperature in different regions with the same mean annual air temperature. For example, points with a mean annual air temperature close to −10 ℃ are characterized by T_{25} values differing by 9 ℃.

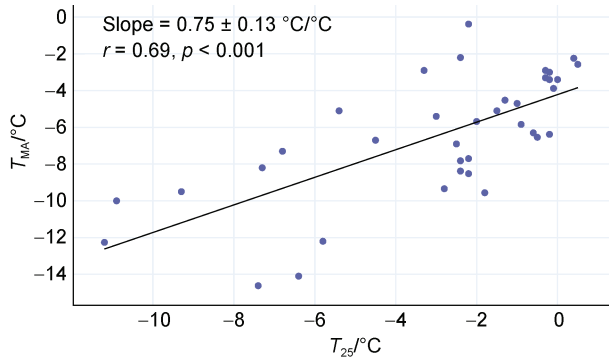

Figure 8 Scatter plot of ground temperature (T_{25}) at depth of 25 m –mean annual air temperature (T_{MA}) for the period 2019–2023 for 38 RNS BPM weather stations. Legend presents values of the slope coefficient, correlation coefficient (r), and significance level (p-value).

5 Conclusions

The RNS BPM aims to serve as country-scale instrument for collecting information about permafrost state, which could be used in global climate models and for regional planning in Russia. By the end of 2025, the permafrost monitoring network will comprise 140 sites covering the entire Russian permafrost zone. The design of the monitoring network is based on long-term permafrost observations combined with monitoring of climatic parameters. This is why RNS BPM boreholes and 50 m × 50 m ALT sites are located in close proximity to weather stations.

As of October 2024, 38 sites have been installed, covering the Northern Sea Route, Yamal region, Norilsk industrial region, Altai–Sayan Mountain region, and Central and Southern Yakutia, with the northernmost location on Franz Josef Land (80.6°N) and southernmost location in the Altai Mountains (49.7°N). For these 38 weather stations, the mean annual air temperature trend for the period 1994–2023 was positive, with the exception of Kosh–Agach in the Altai region. Strong correlation exists between the trend of mean annual air temperature and latitude.

Among the 38 sites, the lowest temperature at the depth of zero annual amplitude (−11.3 ℃) is observed on the New Siberian Archipelago. In the western part of the Eurasian High Arctic, heat flux from the Atlantic leads to higher permafrost temperatures than those found in the cold region between Wiese Island and the New Siberian Archipelago. Higher temperatures on Wrangel Island are attributed to heat flux from the Pacific. Despite lower mean annual air temperatures in some regions of continental Yakutia, permafrost temperatures at the depth of zero annual amplitude are higher than those on Wiese Island and in the New Siberian Archipelago. One of the main explanatory factors regarding such a difference is the effect of high snow density in the High Arctic and lower snow density in continental Yakutia. The major agglomeration with warm background permafrost temperatures close to 0 ℃ is located near the Arctic Circle in Western Siberia. Talik extending down to a depth of 9.8 m was found in the Salekhard borehole. Similarly, talik was found in the borehole in the Altai Mountains near the border with Mongolia, where the upper boundary of permafrost is located at the depth of 5.9–8.9 m. In most of the boreholes with annual measurement cycles, a positive vertical temperature gradient exists below the depth of zero annual amplitude, indicating ongoing warming of the upper part of permafrost attributable to climate change. According to the borehole data, the maximum ALT is observed in September with only two exceptions: the High Arctic sites on Franz Josef Land and Wiese Island and in the low-latitude Sayan Mountain region, where maximum thawing is observed at the end of August. A shallow active layer (minimum: 31 cm on the New Siberian Archipelago) is observed in high-altitude low-temperature permafrost regions. In areas with warm permafrost, ALT variation is higher owing to more pronounced effects of local environmental factors such as vegetation and soil hydrology.

Acknowledgments This work was supported by the Key Innovative Project of National Importance “Unified National System for Monitoring

Climate-active Substances". We specially thank two anonymous reviewers and Associate Editor Dr. Cunde Xiao for their insightful reviewing comments and suggestion.

References

Anisimov O, Zimov S. 2021. Thawing permafrost and methane emission in Siberia: synthesis of observations, reanalysis, and predictive modeling. Ambio, 50(11): 2050-2059, doi: 10.1007/s13280-020-01392-y.

Badina S V, Pankratov A A. 2021. The value of buildings and structures for permafrost damage prediction: the case of eastern Russian Arctic. Geogr Environ Sustain, 14(4): 83-92, doi: 10.24057/2071-9388-2021-058.

Biskaborn B K, Smith S L, Noetzli J, et al. 2019. Permafrost is warming at a global scale. Nat Commun, 10(1): 264, doi: 10.1038/s41467-018-08240-4.

Brown J, Hinkel K M, Nelson F E. 2000. The circumpolar active layer monitoring (CALM) program: Research designs and initial results. Polar Geogr, 24(3): 166-258, doi: 10.1080/10889370009377698.

Burgess M M, Smith S L, Brown J, et al. 2000. Global terrestrial network for permafrost (GTNet-P): permafrost monitoring contributing to global climate observations. Geological Survey of Canada, Current Research 2000-E14, 1-8. http://www.nrcan.gc.ca/gsc/bookstore.

Gruber S. 2012. Derivation and analysis of a high-resolution estimate of global permafrost zonation. Cryosphere, 6(1): 221-233, doi: 10.5194/tc-6-221-2012.

Porfiriev B N, Eliseev D O, Streletskiy D A. 2021. Economic assessment of permafrost degradation effects on the housing sector in the Russian Arctic. Her Russ Acad Sci, 91(1): 17-25, doi: 10.1134/S1019331621010068.

Romanovsky V E, Drozdov D S, Oberman N G, et al. 2010. Thermal state of permafrost in Russia. Permafr Periglac Process, 21(2): 136-155, doi: 10.1002/ppp.683.

Yershov E D (ed.). 1996. Geocryologic Map of the USSR, Scale 1:2, 500,000 Million. Vinnytsia: State Cartographic Factory, Ukraine (in Russian).